Proceedings of the
44th IEEE Conference on Decision and Control, and
the European Control Conference 2005
Seville, Spain, December 12-15, 2005

Forced Oscillations of a Membrane with Quadratic Nonlinearity

Andras Balogh and Vladimir Varlamov

Abstract— **This paper deals with a forced, damped Boussinesq equation on the unit circle with quadratic nonlinearity, which represents small nonlinear oscillations of an elastic membrane in the presence of viscosity. We use the eigenfunction expansion method in order to construct global–in–time solutions with well–established convergence properties in Sobolev spaces. Existence and uniqueness follow from the construction. Numerical examples with the adaptation of the theoretical method show the viability of the method.**

I. INTRODUCTION

The present work is concerned with the problem of response of an elastic membrane to an incident acoustic wave (Fig. 1). This issue appears in the context of studying acoustic detection via registering vibrations of thin elastic structures [1], [2]. In particular, the necessity of creation of passive sensor technologies determines the importance of the study of oscillations of elastic membranes under the influence of acoustic fields. Unattended acoustic ground sensors can have as their basic element a membrane with fixed ends (clamped, simply supported or even nonlinearly damped).

The so called "good" Boussinesq equation is well known in the context of governing small nonlinear oscillations of elastic beams. This equation can be written in the form (see [3])

$$u_{tt} = -\alpha u_{xxxx} + u_{xx} + \beta \left(u^2\right)_{xx}, \tag{1}$$

where $\alpha = const > 0$ is the dispersion parameter depending on the compression and rigidity characteristics of the material, $\beta = const \in \mathbb{R}$ is the constant coefficient controlling nonlinearity (it can be set equal to one by appropriate scaling, but it is convenient to keep it in order to trace the influence of nonlinearity) and $u(x,t)$ is the vertical deflection. The quadratic nonlinearity appearing in (1) accounts for the curvature of the bending beam.

Equation (1) with $\alpha < 0$ is known as the "bad" Boussinesq equation since it possesses linear instability. It describes the propagation of long surface waves on shallow water. A two-dimensional "bad" Boussinesq equation

$$u_{tt} = u_{xxxx} + u_{xx} + u_{yy} + 3\left(u^2\right)_{xx} \tag{2}$$

was introduced in [4] to describe the propagation of gravity waves on the surface of water, in particular the head–on collision of oblique waves. An initial–value problem for the "bad" Boussinesq equation with a potential

$$u_{tt} = 3\Delta^2 u + \Delta u - 12\left(V(x) * \Delta(|u|^\lambda u)\right), \qquad x \in \mathbb{R}^2,\ t > 0,$$

was considered in the paper [5]. For small initial data, $\lambda > 8$ and sufficiently smooth potential $V(x)$ it was shown that there exists a global solution satisfying the decay estimate $\|u(\cdot,t)\|_{L_\infty} \le c(1+t)^{-7}$.

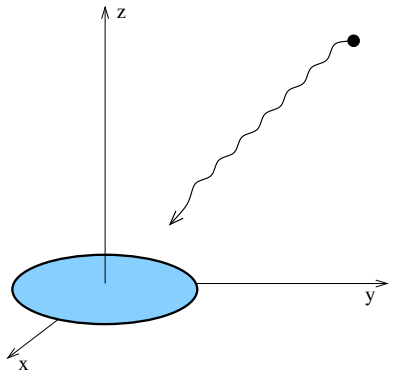

Fig. 1. Circular membrane with incident wave.

A convenient item responsible for internal friction and related to heat generation, is $-2bu_{txx}$, where $b = const > 0$. After adding it to the left-hand side of (1) the equation becomes

$$u_{tt} - 2bu_{txx} = -\alpha u_{xxxx} + u_{xx} + \beta\left(u^2\right)_{xx}. \tag{3}$$

A two-dimensional analog of (3) (sometimes called a damped plate equation) is

$$u_{tt} - 2b\Delta u_t = -\alpha\Delta^2 u + \Delta u + \beta\Delta(u^2), \tag{4}$$

where α, $b = const > 0$, $\Delta = \partial_x^2 + \partial_y^2$, $\Delta^2 = \Delta\Delta$ and $u(x,y,t)$ is the vertical deflection of a membrane. It appears in the context of modeling small nonlinear oscillations of elastic membranes. A "uniform" nature of this equation contrasts with that of its "asymmetric" counterpart (2) from the theory of water waves.

Equation (4) with distributed forcing is the main topic of our paper. The paper is organized as follows. In Section II the main initial–boundary–value problem is posed, notations are introduced, function spaces are defined and main theoretical results are described. Section III with numerical simulations forms the main part of the paper. We explain the computational adaptation of the eigenvalue expansion method, present a short conceptual comparison with other numerical methods and provide numerical examples. The examples demonstrate some of the theoretical convergence properties of the method, show some extension to the theory, and provide insight to the longtime asymptotics of solutions.

0-7803-9568-9/05/$20.00 ©2005 IEEE

II. PROBLEM STATEMENT AND MAIN RESULTS

Denote by Ω a disk of a unit radius and put the origin of the coordinate system in its center, so that in polar coordinates $\Omega = \{(r,\theta) : |r| < 1,\ \theta \in [-\pi,\pi]\}$. Let $\partial\Omega$ be its boundary. Our purpose is to consider the following initial–boundary–value problem for the real function $u = u(r,\theta,t)$

$$\begin{gathered} u_{tt} - 2b\Delta u_t = -\alpha\Delta^2 u + \Delta u + \beta\Delta(u^2) + af(r,\theta,t), \\ u|_{\partial\Omega} = \Delta u|_{\partial\Omega} = 0, \\ u(r,\theta,0) = u_t(r,\theta,0) = 0, \\ u(r,\theta+2\pi,t) = u(r,\theta,t), \\ \text{for } (r,\theta) \in \Omega,\ t > 0, \\ \text{boundedness of } u \text{ at the origin,} \end{gathered} \tag{5}$$

where α, b and a are positive constants, β is a real constant, Ω denotes the unit disk, and $\partial\Omega$ is its boundary, the unit circle. The parameter a controls the forcing term and must be bounded in order to guarantee convergence of series (15) below. Therefore acoustic pressure is expected to be not too big in the framework of the current model. Large nonlinear oscillations will be considered below only numerically, and in our future work theoretically using different membrane models. The above boundary conditions correspond to a simply supported boundary (see [6]).

We restrict our attention to the most interesting case $\alpha^2 > b^2$ of small damping which corresponds to the existence of an infinite number of damped oscillations. If the inverse relation holds (the so called overdamping case), aperiodic processes play the main role.

We seek solutions of the problem (5) in the form of the eigenfunction expansion

$$u(r,\theta,t) = \sum_{m=-\infty}^{\infty}\sum_{n=1}^{\infty} \hat{u}_{mn}(t)\Phi_{mn}(r,\theta) \tag{6}$$

with the main task being to find the coefficients $\widehat{u}_{mn}(t)$, and where

$$\Phi_{mn}(r,\theta) = J_m(\lambda_{mn} r)e^{im\theta}, \quad m \in \mathbb{Z},\ n \in \mathbb{N} \tag{7}$$

are eigenfunctions of the Laplace operator in a disk, i.e. solutions to the eigenvalue problem

$$\Delta\Phi(r,\theta) = -\Lambda\Phi(r,\theta), \qquad (r,\theta) \in \Omega, \tag{8}$$

$$\Phi|_{\partial\Omega} = 0, \quad \Phi(r,\theta+2\pi) = \Phi(r,\theta), \tag{9}$$

$$|\Phi(0,\theta)| < \infty. \tag{10}$$

In this way we can satisfy the boundary conditions, periodic conditions in θ and the boundedness condition for u. The functions J_m are Bessel functions of index m for $m \in \mathbb{N}$. In order to satisfy the boundary conditions $\{\lambda_{mn}\}_{n=1}^{\infty}$ should be positive zeros of the dispersion equation

$$J_m(\lambda) = 0 \quad \text{for } m \in \mathbb{Z}.$$

Our choice of the boundary condition simplifies the dispersion relation. So far our approach resembles the classical method of separation of variables, but now the necessity to solve the nonlinear equation brings new ideas into consideration.

The sequence $\{\Phi_{mn}\}_{m\in\mathbb{Z},n\in\mathbb{N}}$ forms a complete orthogonal set in $L_2(\Omega)$. Expanding the source term of the equation into the series of the (6) type we obtain

$$f(r,\theta,t) = \sum_{m=-\infty}^{\infty}\sum_{n=1}^{\infty} \hat{f}_{mn}(t)\Phi_{mn}(r,\theta).$$

Using notations $\langle\cdot,\cdot\rangle$ and $\|\cdot\|$ for the L_2–inner product and norm respectively we have

$$\hat{f}_{mn}(t) = \frac{< f, \Phi_{mn} >}{\|\Phi_{mn}\|^2}. \tag{11}$$

In this paper we use the assumption that

$$\left|\hat{f}_{mn}(t)\right| \le \hat{f}_* \sqrt{\lambda_{mn}} e^{-\kappa t},$$

where $\hat{f}_*$ and κ are constants and $0 \le 2\kappa < b\lambda_{01}^2$.

We obtain the following nonlinear initial value problem for the coefficients $\hat{u}_{mn}(t)$ with $m \in \mathbb{Z}$, $n \in \mathbb{N}$

$$\begin{aligned} \hat{u}''_{mn}(t) + 2b\lambda_{mn}^2\hat{u}'_{mn}(t) + (\alpha\lambda_{mn}^4 + \lambda_{mn}^2)\hat{u}_{mn}(t) \\ = -\beta\lambda_{mn}^2\widehat{u^2}_{mn}(t) + a\hat{f}_{mn}(t),\ t > 0, \\ \hat{u}_{mn}(0) = \hat{u}'_{mn}(0) = 0, \end{aligned} \tag{12}$$

where the coefficients of the eigenfunction expansion of the nonlinearity are calculated by the formulae

$$\begin{aligned} \widehat{u^2}_{mn}(t) &= \frac{1}{\|\Phi_{mn}\|^2}\left\langle \sum_{p,q}\hat{u}_{pq}(t)\Phi_{pq} \cdot \sum_{k,s}\hat{u}_{ks}(t)\Phi_{ks}, \Phi_{mn}\right\rangle \\ &= \sum_{p,q,k,s} b(m,n;p,q,k,s)\hat{u}_{pq}(t)\hat{u}_{ks}(t), \end{aligned}$$

and

$$b(m,n,p,q,k,s) = \frac{< \Phi_{pq}\cdot\Phi_{ks}, \Phi_{mn} >}{\|\Phi_{mn}\|^2}. \tag{13}$$

Integrating (12) with respect to t we get the nonlinear integral equation

$$\begin{aligned} \hat{u}_{mn}(t) = \frac{a}{\sigma_{mn}}\int_0^t e^{-b\lambda_{mn}^2(t-\tau)}\sin\left[\sigma_{mn}(t-\tau)\right]\hat{f}_{mn}(\tau)d\tau \\ - \frac{\beta\lambda_{mn}^2}{\sigma_{mn}}\int_0^t e^{-b\lambda_{mn}^2(t-\tau)}\sin\left[\sigma_{mn}(t-\tau)\right]\widehat{u^2}_{mn}(\tau)d\tau, \end{aligned} \tag{14}$$

where

$$\sigma_{mn} = \lambda_{mn}\sqrt{\mu\lambda_{mn}^2 + 1} \quad \text{and} \quad \mu = \alpha - b^2 > 0.$$

For solving (14) we apply the perturbation theory. We seek its solution in the form

$$\hat{u}_{mn}(t) = \sum_{N=0}^{\infty} a^{N+1}\hat{v}_{mn}^{(N)}(t). \tag{15}$$

Substituting (15) into equation (14) we obtain the recursion formulas

$$\hat{v}_{mn}^{(0)}(t) = \frac{1}{\sigma_{mn}}\int_0^t e^{-b\lambda_{mn}^2(t-\tau)}\sin\left[\sigma_{mn}(t-\tau)\right]\hat{f}_{mn}(\tau)d\tau, \tag{16}$$

$$\begin{aligned} \hat{v}_{mn}^{(N)}(t) = -\frac{\beta\lambda_{mn}^2}{\sigma_{mn}}\int_0^t e^{-b\lambda_{mn}^2(t-\tau)}\sin\left[\sigma_{mn}(t-\tau)\right] \\ \times \sum_{p,q,k,s} b(m,n,p,q,k,s)\sum_{j=1}^{N}\hat{v}_{pq}^{(j-1)}(\tau)\hat{v}_{ks}^{(N-j)}(\tau)d\tau \end{aligned} \tag{17}$$

for $N \geq 1$.

We need the concept of mild solutions in order to formulate our main theorem. Integration of the equation (5) with respect to t leads to a nonlinear integral equation which serves for the definition of a mild solution of the problem (5). Denote by A the operator $-\Delta$ defined on sufficiently smooth functions $\Phi(r,\theta)$ satisfying the Dirichlet and periodic boundary conditions (9) and let

$$\sigma(A) = (\mu A^2 + A)^{1/2} \qquad \text{where} \qquad \mu = \alpha - b^2 > 0.$$

Definition. A function $u(t)$ is called a *mild solution* of the problem (5) if it satisfies the integral equation

$$u(t) = a\int_0^t e^{-b(t-\tau)A}(\sigma(A))^{-1}\sin(\sigma(A)(t-\tau))f(\tau)d\tau - \beta\int_0^t e^{-b(t-\tau)A}(\sigma(A))^{-1}\sin(\sigma(A)(t-\tau))Au^2(\tau)d\tau$$

in the Banach space $C(\mathbb{R}^+, H_0^s(\Omega))$.

Using this definition and the above construction we arrive at the following main theorem on the existence and uniqueness of solutions.

If $\alpha > b^2$, $f \in C_b(\mathbb{R}^+,\ L_2(\Omega))$, and $a < 3\mu\left(b\lambda_{01}^2 - \kappa\right)^2 / \left[2\pi^2|\beta|\lambda_{01}^4 \hat{f}_*\right]$, then there exists a mild solution $u \in C_b\left(\mathbb{R}^+, H_0^s(\Omega)\right)$, $s < 3/2$, of the problem (5). For $-1 < s < 3/2$ this solution is unique. It can be represented in the form of a series

$$u(r,\theta,t) = \sum_{m,n} \hat{u}_{mn}(t) J_m(\lambda_{mn} r) e^{im\theta}, \tag{18}$$

where the coefficients $\hat{u}_{mn}(t)$ are defined by (15), (16) and (17) and convergence is understood in the sense of $H^s(\Omega)$. The Sobolev s–norm of the solution satisfies the estimate

$$\|u(\cdot,t)\|_s^2 \leq C\sum_{m,n} R^2(m)\lambda_{mn}^{2s-4} = O\left(\sum_m \frac{\ln^2 m}{m^2}\sum_n \frac{1}{(m+2n)^{4-2s}}\right) < \infty. \tag{19}$$

The proof of this theorem will be presented in details in our forthcoming paper.

III. NUMERICAL RESULTS

In this section we use the eigenfunction method of Section II for numerical simulations. In fact, we use a straightforward numerical adaptation of this approach. In our future work we will optimize the numerical method for speed and accuracy.

We used FORTRAN95 with IMSL and CERNLIB subroutines for numerical calculations, and MATLAB 6.5 for visualization on a LINUX workstation with dual 2GHz processors and 2GB memory.

A. The numerical procedure

The numerical procedure, based on (15), (16), (17) and (18) consists of the following main steps:

1) Calculate the Fourier–Bessel coefficients of the forcing term using the formula

$$\hat{f}_{mn}(t) = \frac{< f, \Phi_{mn} >}{\|\Phi_{mn}\|^2} \tag{20}$$

where $m = -\widetilde{M}, \ldots \widetilde{M}$, and $n = 1, \ldots, \widetilde{N}$ for given $\widetilde{M}$, $\widetilde{N}$, $\in \mathbb{N}$. The integrations in polar coordinates require discretization. We used simple Riemann sums in polar coordinates with constant dr and $d\theta$ mesh sizes.

2) Calculate the nonlinear coefficients

$$b(m,n;p,q,k,s) = \frac{< \Phi_{pq}\cdot\Phi_{ks}, \Phi_{mn} >}{\|\Phi_{mn}\|^2} \tag{21}$$

where $m = -\widetilde{M}, \ldots \widetilde{M}$, $n = 1, \ldots, \widetilde{N}$. While the total number of terms is $\left(\widetilde{M}+1\right)^3 \widetilde{N}^3$, due to orthogonality, $b(m,n;p,q,k,s) \neq 0$ only if $p+k=m$. This reduces the number of nonzero terms to $\left(\widetilde{M}+1\right)^2 \widetilde{N}^3$. Further reduction in storage can be achieved by using the symmetry of the terms.

3) Calculate the perturbation series recursively

$$\hat{v}_{mn}^{(0)}(t) = \int_0^t e^{-b\lambda_{mn}^2(t-\tau)} \frac{\sin\left[\sigma_{mn}(t-\tau)\right]}{\sigma_{mn}} \hat{f}_{mn}(\tau)d\tau, \tag{22}$$

$$\hat{v}_{mn}^{(l)}(t) = -\frac{\beta\lambda_{mn}^2}{\sigma_{mn}}\int_0^t e^{-b\lambda_{mn}^2(t-\tau)}\sin\left[\sigma_{mn}(t-\tau)\right] \times \sum_{p,q,k,s}^{*} b(m,n,p,q,k,s)\sum_{j=1}^{l}\hat{v}_{pq}^{(j-1)}(\tau)\hat{v}_{ks}^{(l-j)}(\tau)d\tau \tag{23}$$

for $l = 1, \ldots, N_v$, $t \in [0,T]$, $m = -\widetilde{M}, \ldots \widetilde{M}$ and $n = 1, \ldots, \widetilde{N}$. This part is the most demanding computationally, requiring the evaluation of convolution type integrals and 5 sums embedded in the integral. In order to keep computational costs minimal we used Simpson's method for the approximation of the convolution with constant time step size dt. Subsection III-C shows that even this rudimentary quadrature gives good results.

4) Assemble the Fourier–Bessel coefficients of the solution

$$\hat{u}_{mn}(t) = \sum_{l=0}^{Nv} a^{l+1}\hat{v}_{mn}^{(l)}(t) \tag{24}$$

at all gridpoints t. This part is trivial.

5) Assemble the solution

$$u(r,\theta,t) = \sum_{m=0}^{\widetilde{M}}\sum_{n=1}^{\widetilde{N}} \hat{u}_{mn}(t) J_m(\lambda_{mn} r) e^{im\theta} \tag{25}$$

at gridpoints t, r, θ.

Certain values related to special functions can be calculated in advance. One set of these quantities is the truncated set of zeros for the Bessel functions: $\{\lambda_{mn}\}_{m,n=01}^{\widetilde{M},\widetilde{N}}$. In order to approximate these zeros we used the CERNLIB subroutine DBZEJY, which is based on an iterative method by Temme [7]. Another sequence of quantities consists of the squared L_2–norms of the eigenfunctions

$$\left\{\|\Phi_{mn}\|^2\right\}_{m,n=-\widetilde{M},1}^{\widetilde{M},\widetilde{N}} = \left\{2\pi\int_0^1 r J_m^2(\lambda_{mn} r)\, dr\right\}_{m,n=-\widetilde{M},1}^{\widetilde{M},\widetilde{N}} \tag{26}$$

with symmetry property $\|\Phi_{mn}\| = \|\Phi_{-mn}\|$.

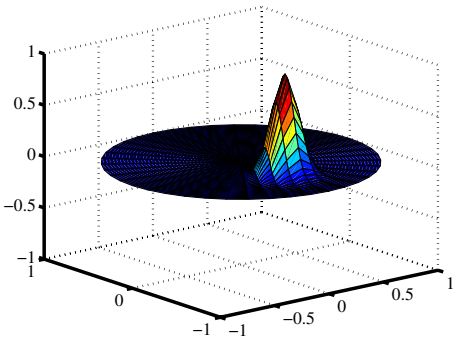

Fig. 2. Forcing function at time $t = 0$ with $\kappa = 0$ (no decay).

B. Comparison with Other Possible Numerical Methods

It will be the topic of future research to compare, through numerical examples, the convergence properties of the algorithm in question with those of other numerical methods. However, we would like to emphasize already here that a unique property of the eigenfunction method (compared to others) is that (19) provides us with a better understanding of the convergence rate of approximations for the *nonlinear* problem (5). While the eigenfunction expansion method is sometimes mistaken for the Galerkin method, the difference is significant. The latter one is based on projection onto the finite–dimensional space of eigenvectors, while the eigenfunction expansion method utilizes projection onto an infinite–dimensional space of eigenvectors with the subsequent detailed analysis of decay of the coefficients of the corresponding series. Using Galerkin's method one obtains the existence of a *convergent subsequence of approximating solutions* based on compactness argument. For nonlinear problems, there is a coupling in the ODEs ((12) in our case), and hence Galerkin's method does not provide a guarantee that in numerical simulations the next approximating solution is better than the previous. Convergence has to be "checked" numerically by repeated refinement of the approximation. Our method *constructs* the solution in the form of *one* absolutely convergent infinite series (18) with decreasing terms (19).

In general for nonlinear problems the other standard methods, like the pseudo spectral approach [8], have similar convergence properties to that of Galerkin's method. Of course, in actual numerical simulation we can encounter different convergence properties than the theoretical ones.

C. Discretization errors and convergence properties

A clear advantage of this method is that there is no modeling error involved. Errors are arising only in the discretization steps and from the truncations of infinite series. Our approach has several of both. A distinctive property of the method is that by working in the Fourier–Bessel space the spatial discretization appears only in the initial (20), (21), (26) and final (25) phases of the algorithm. Also, there is no explicit numerical differentiation involved.

The forcing term is the spatially localized function

$$f(r,\theta,t) = \cos(10\pi t)\exp\left\{-50\left[1/4 + r^2 - r\cos(\theta)\right]\right\} \quad (27)$$

for $t \geq 0$, $r \in [0,1]$ and $\theta \in [0,2\pi]$, depicted in Figure 2 for initial time $t = 0$. The parameter values used in this section are $\alpha = 1$, $\beta = 1$, and $b = 0.9$. We estimate the upper bound on the perturbation parameter a of Theorem II as $a < 7.064 \times 10^{-1}$. The value used is $a = 0.35$ in this subsection.

For the spatial discretization we used $Nr = Nth = 40$ grid points both in the radial and the angular directions. In the time discretization $Nt = 200$ time steps were taken of the size $dt = 10^{-2}$. We demonstrate briefly the convergence properties of the two partial sums (24) and (25) only. We doubled the number of zeros $\widetilde{N}$, the number of Bessel functions $\widetilde{M}$ and the number of terms in (24) N_v from $\widetilde{M} = \widetilde{N} = N_v = 5$ to 10 and then we further increased these values from 10 to 15. These numbers correspond to $\widetilde{M}\widetilde{N} = 25$, 100, and 225 number of terms in the finite sum (25).

Note that in the numerical application of Galerkin's method (both of spectral and of finite element type) it is usual to have a relatively low number of basis functions when one solves the second order nonlinear system of ODEs (12). The main reason for this is the high computational cost of solving nonlinear systems of ODEs and the usually good convergence property of Galerkin's methods observed numerically. In our case the good convergence property is proven in Theorem II.

The obtained numerical solutions are denoted by u_1, u_2, and u_3 for $\widetilde{M} = \widetilde{N} = N_v = 5$, 10 and 15 respectively. The results are summarized in Figure 3. In the second column of the figure we plot the maximum change between the two numerical approximations, i.e.,

$$\Delta u(t) = \max_{(r,\theta)\in\Omega} |u_i(r,\theta,t) - u_{i+1}(r,\theta,t)|,\ t \in [0,2],\ i = 1,2.$$

In the third column of the figure we plot the relative change (in percentage) between the two numerical approximations, i.e.,

$$\%\Delta u(t) = 100\frac{\max_{(r,\theta)\in\Omega} |u_i(r,\theta,t) - u_{i+1}(r,\theta,t)|}{\max_{(r,\theta)\in\Omega} |u_i(r,\theta,t)|}$$

for $t \in [0,2]$, $i = 1,2$. Since we are working with small oscillations, comparing the absolute changes of 8×10^{-6} and 10^{-7} in solutions is not descriptive. Comparing the relative changes we observe in the last column of Figure 3 the following features: After doubling the three discretization parameters $\widetilde{M}$, $\widetilde{N}$ and N_v from 5 to 10 there appears about 8% change in the solutions, and a further increase of the aforementioned discretization parameters from 10 to 15 results in less than 0.12% change in the solution, which we consider to be very small.

D. Nonlinear oscillations

We emphasize that (5) models *small* nonlinear oscillations of certain uniform elastic membranes. However, in this section we use parameter values for which oscillations are relatively large, and hence the nonlinear term has a prominent

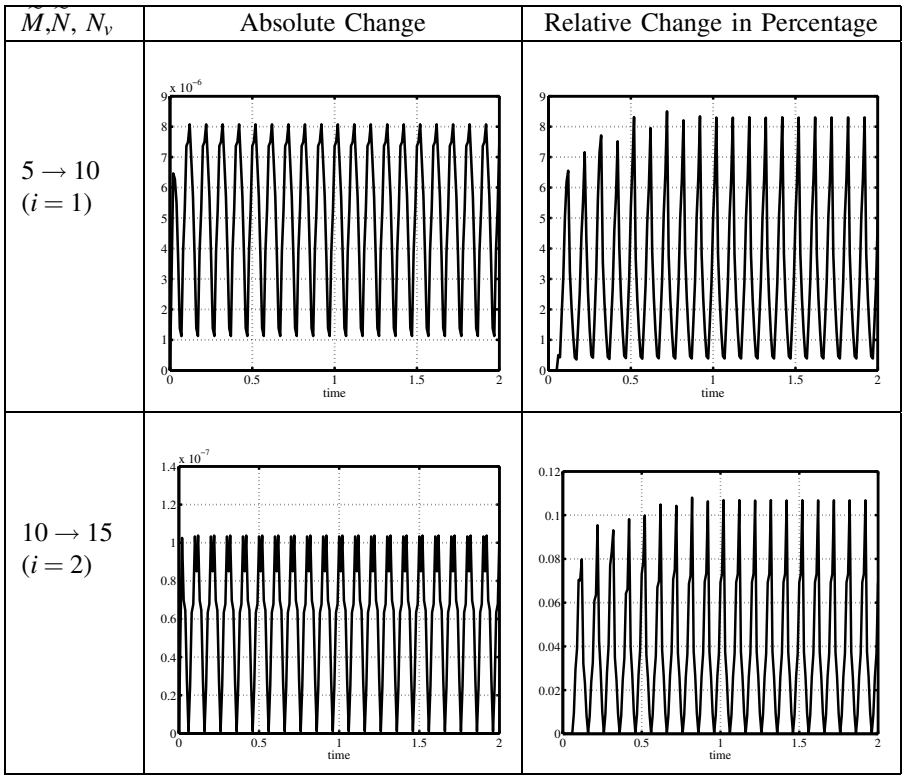

Fig. 3. Maximum change in the approximations as $\widetilde{M}$, $\widetilde{N}$ and N_v are increased from 5 to 10 and from 10 to 15.

effect on the solution. The parameter values are now $\alpha = 0.1$, $a = 700$ and $b = 0.1$. The damping is small and oscillations are strong.

We present a comparison of the linear $(\beta = 0)$ and strongly nonlinear $\left(\beta = 10^3\right)$ membrane oscillations under forcing (27). In Figure 4 we plotted the maximum vertical deflection of the membrane under and above the horizontal plane for the linear and nonlinear cases respectively. The extreme values of the solution are vertically symmetric and oscillations seem to be periodic in time for the linear membrane. In the nonlinear case the extreme values are skewed downward and there is no time periodicity.

Figure 5 shows the linear and nonlinear membranes at various time instants. The strong nonlinear effects are clearly visible in the second column of the table. An interesting consequence of the periodic forcing in the linear case is that oscillations seem to be periodic with the shape of the membrane being the same for $t = 1.75$ and $t = 3.15$. We did not observe such periodicity in the nonlinear case.

The finite series

$$\hat{u}_{mn}(t) = \sum_{l=0}^{Nv} a^{l+1} \hat{v}_{mn}^{(l)}(t) \tag{28}$$

approximating the Fourier–Bessel coefficients of the solution shows good convergence properties even for the case of large perturbation parameter $a = 700$ (see Table I). Stopping after a relatively small number of iterations ($N_v = 15$) is reasonable not just due to the fast convergence but also because for large iteration index l and large perturbation parameter a the multiplication of the large number a^{l+1} and the small number $\hat{v}_{mn}^{(l)}(t)$ is numerically unstable.

TABLE I
CONVERGENCE PROPERTIES OF SERIES $\hat{u}_{mn}(t) = \sum_{l=0}^{Nv} a^{l+1} \hat{v}_{mn}^{(l)}(t)$

l	a^{l+1}	$\max_{m,n,t} \left\lvert \hat{v}_{mn}^{(l)}(t) \right\rvert$	$a^l \max_{m,n,t} \left\lvert \hat{v}_{mn}^{(l)}(t) \right\rvert$
0	$7.00E+02$	$1.25E-04$	$8.75E-02$
2	$3.43E+08$	$1.46E-12$	$5.01E-04$
4	$1.68E+14$	$1.39E-20$	$2.34E-06$
6	$8.24E+19$	$3.05E-28$	$2.51E-08$
8	$4.04E+25$	$4.65E-36$	$1.88E-10$
10	$1.98E+31$	$4.49E-44$	$8.88E-13$

IV. Conclusions and Future Works

A. Conclusions

The eigenfunctions expansion method was developed for a forced nonlinear Boussinesq equation representing forced, small and nonlinear oscillations of an elastic membrane. The method was used for numerical simulations. The numerical algorithm required several levels of approximations. All these steps were tested for convergence. The convergence properties show that the eigenfunction expansion is a viable alternative to other numerical methods.

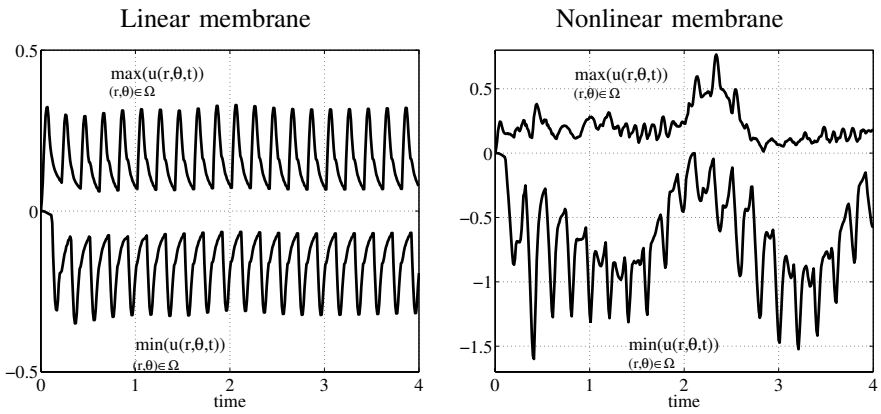

Fig. 4. Extreme values of linear and nonlinear membrane oscillations.

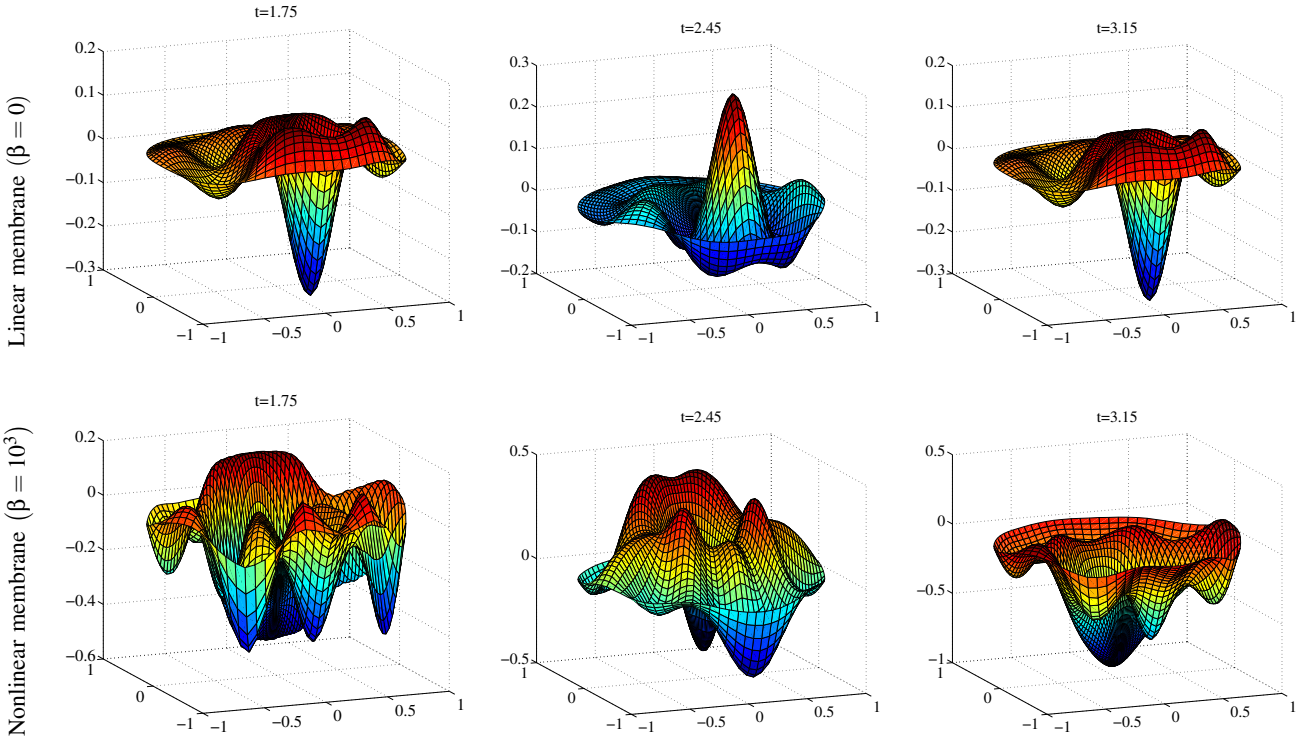

Fig. 5. Linear and nonlinear membrane oscillations.

B. Future Work

In the future we plan to investigate the long time asymptotics of the nonlinear forced membrane oscillations for specific forcing functions. In order to describe large nonlinear oscillations of a membrane we are going to consider the general Föppl–von Kármán system [9].

REFERENCES

[1] C. Jenkins and J. Leonard, "Nonlinear dynamic response of membranes: State of the art," *Appl. Mech. Rev.*, vol. 44, no. 7, pp. 319–328, 1991.

[2] O. Rudenko and S. Soluyan, *Theoretical Foundations of Nonlinear Acoustics*. Moscow, Nauka, 1975.

[3] J. Bona and L. Luo, "More results on the decay of solutions to nonlinear dispersive wave equations," *Discrete and Continuous Dynamical Systems*, vol. 1, pp. 151–193, 1995.

[4] R. Johnson, "A two–dimensional boussinesq equation for water waves and some of its solutions," *J. FLuid Mech*, vol. 323, pp. 65–78, 1996.

[5] D. Akmel, "Global existence and decay for solutions to the "bad" boussinesq equation in two space dimensions," *Appl. Anal.*, vol. 83, no. 1, pp. 17–36, 2004.

[6] L. Landau and E. Lifshitz, *Theory of Elasticity*. Addison–Wesley, Inc., London, 1959.

[7] N. Temme, "An algorithm with algol60 program for the computation of the zeros of ordinary bessel functions and those of their derivatives," *J. Comput. Phys.*, vol. 32, pp. 270–279, 1979.

[8] J. Boyd, *Chebyshev and Fourier Spectral Methods*, 2nd ed. New York: Dover Publications, 2000.

[9] A. Föppl, *Vorlesungen ü. Technische Mechanik*. Leipzig, 1907, bd. 5.